A Time-Dependent Density Functional Theory Investigation of the Spectroscopic Properties of the *β*-Subunit in C-Phycocyanin

Yanliang Ren and Jian Wan*

Key Laboratory of Pesticide & Chemical Biology (CCNU), Ministry of Education, Department of Chemistry, Central China Normal University, Wuhan 430079, China

Xin Xu*

State Key Laboratory for Physical Chemistry of Solid Surfaces, College for Chemistry and Chemical Engineering, Center for Theoretical Chemistry, Xiamen University, Xiamen 361005, China

Qingye Zhang and Guangfu Yang

College of Chemistry, Central China Normal University, Wuhan 430079, China

Received: July 25, 2006

By using time-dependent density functional theory combined with the polarizable continuum model, a satisfactory assignment of the absorption and circular dichroism spectra and energy transfer flow of the *β*-subunit in C-phycocyanin (C-PC) was achieved when the protonation of *β*-84 and *β*-155 phycocyanobilin (PCB) and their interaction with the protein moiety in C-PC have been taken into account. We attribute the main peak for both *β*-84 and *β*-155 as arising from the *π* electron excitation of the pyrrole rings and the shoulder peak as arising from the charge transfer from the asparate residue to $PCBH^+$. The satisfactory agreement between theory and experiment suggests that Förster resonance theory prevails such that energy transfer occurs from β_s (*β*-155) to β_f (*β*-84).

I. Introduction

Open-chain tetrapyrrolic chromophores play a crucial role in biological photoreceptors.[1] Phytochromes, in both the photomorphogenic pigments of green plants, and phycobiliproteins, the light-harvesting pigments in the photosynthetic apparatus of some algae, contain at least one open-chain tetrapyrrolic chromophore that is covalently bonded by a thioether linkage to a protein moiety.[1] The biological action of these photoreceptors is based on the photophysical and photochemical processes occurring after the absorption of light in their tetrapyrrolic chromophores. In view of this fact, studies on the photochemistry and photophysics of tetrapyrrole compounds have gained increasing attention in the past decade.[1,2]

C-phycocyanin (C-PC) is an important component of phycobilisomes. It was found as a complex solution of trimers ($\alpha_3\beta_3$), hexamers ($\alpha_6\beta_6$), and other oligomers, where each α polypeptide subunit has one chromophore known as phycocyanobilin (PCB, a derivative of an open-chain tetrapyrrole) and each *β*-subunit has two PCBs.[1] The sequence of the amino acids for C-PC is clear, where PCBs are located at α-84, *β*-84, and *β*-155, respectively.[3−5] Schematic representation of a C-PC monomer is shown in Figure 1.

To make clear the elementary processes in light harvesting and energy migration by C-PC of phycobilisomes, knowledge of the electronic ground states and the excitation states of PCBs is a prerequisite. Mimuro and co-workers did a thorough spectroscopy study[5,6] for C-PC isolated from cyanobacterium *Mastigocladus laminosus*.[7] They reported the detailed absorption and circular dichroism (CD) spectra for not only monomer ($\alpha\beta$) and trimer ($\alpha_3\beta_3$) of C-PC but also the α- and *β*-subunits,[5] thus laying a solid experimental foundation for further theoretical investigation.

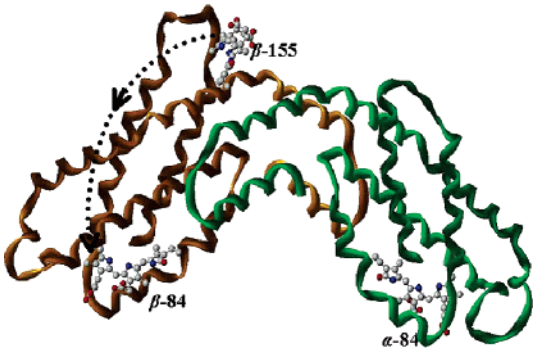

Figure 1. Schematic representation of a C-phycocyanin monomer. The green chain is the α-subunit and the brown chain is the *β*-subunit.

Previously, we studied the absorption and CD spectra of the α-subunit in C-PC by using time-dependent density functional theory (TDDFT).[8] Satisfactory results were obtained after the chromophore−protein interactions were properly taken into account. While the polarizable continuum model (PCM) disclosed the importance of the long-range interaction between the chromophore and the protein pocket, the short-range interaction was strongly signified by the protonation of the ring C nitrogen such that both ring B and ring C nitrogens hydrogen-bonded to the asparatate residues (cf. Figure 2).[8] In the present work, we have extended our study of the α-subunit to the *β*-subunit. To our knowledge, except one semiempirical calculation,[7] no

* Corresponding authors. E-mails: jianwan@mail.ccnu.edu.cn; xinxu@xmu.edu.cn.

10.1021/jp064734v CCC: $33.50
Published on Web 08/23/2006

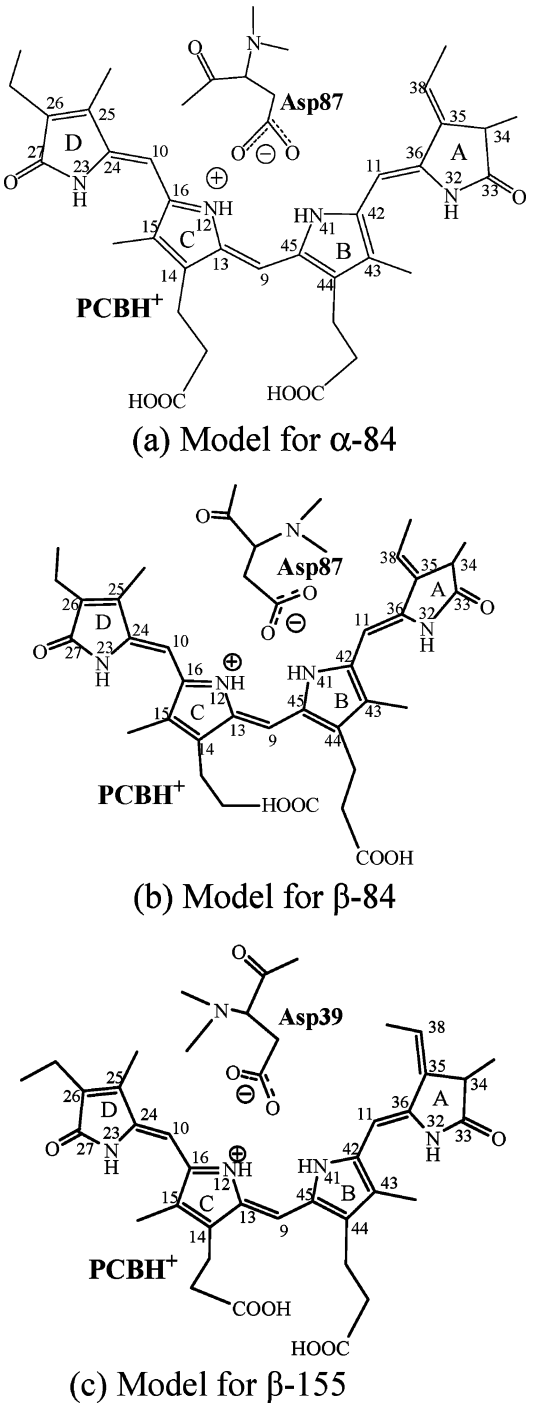

Figure 2. Model complexes consisting of $PCBH^+$ and the asparate residue for the α-84, *β*-84, and *β*-155 PCBs, respectively.

previous first-principle study is available for the absorption and CD spectra of the *β*-subunit.

The present paper is organized as follows. In section II, we outline the computational details. Calculation results and discussions are presented in section III. A summary is given in section IV.

II. Computational Details

Several biliprotein crystals have been characterized.[9,10] The present calculations adopted the three-dimension geometric parameters of backbone taken from the crystal structures of C-PC (1CPC in the Protein Data Bank at the Brookhaven National Laboratory), which was isolated from the cyanobacterium *Fremyella diplosiphone* (resolution of 1.66 Å),[10] in which the geometries of PCBs were found to be similar to those of the earlier crystal data from *M. laminosus* (resolution of 2.1 Å) and *Agmenellum quadruplicatum* (resolution of 2.5 Å).[10] The hydrogen atoms were carefully added by using GaussView 3.07.[11] The N-terminus was set to $-N(CH_3)_2$, while the C-terminus $-COOH$ was replaced with $-COCH_3$ for the asparatate residue, due to the O atom in the $-OH$ group strongly attracting electrons. At the C-terminus of C-PC, the $-COOH$ was used (cf. Figure 2). Although the crystal structure[9,10] is unable to show evidence for protonation, our previous calculations demonstrate that protonation is most likely existing in the α-84 chromophore.[8] Thus, in the present calculations of *β*-84 and *β*-155, we have also adopted this $PCBH^+$-Asp model (Figure 2).

The surrounding protein moiety was taken as a polarizable solvent media described by PCM,[14] whose reliability for both ground and excited states is now well-documented.[8,14,15] In the present calculations, we use $\epsilon = 4.0$ as suggested by Blomberg and co-workers for their study of charge separation in *Rhodobacter sphaeroides* bacteria and Photosystem II in green plants.[15] We performed full geometry optimizations of the model complexes using the B3LYP flavor[12] of DFT,[12] with a 6-31G*[13] basis set in PCM. For each optimized geometry, vibrational frequencies are calculated analytically to ensure it to be a true local minimum. The vertical singlet→singlet excited states of the model complexes were calculated by using the TDDFT method at the 6-31+G(d) level.

Additional calculations were performed to decompose the influencing effects. (1) We have optimized the geometries in vacuo and calculated the absorption and CD spectra in PCM with these geometries. Comparison with these results shows how solvent effect will influence the geometries to affect the spectra.[16] (2) We have performed TDDFT calculations with and without use of PCM at a given geometry. These results signify the importance of the long-range interaction from the protein environment on the spectra. (3) We have also examined the importance of the short-range interaction from the protein environment. The models for comparisons included a neutral PCB or a protonated PCB with or without taking the nearby asparatate residue into account.

All calculations were performed by using the Gaussian 03 suite of programs[11] on a SGI/Origin-300 server.

III. Results and Discussion

A. Geometric Parameters. The optimized geometries of *β*-84 and *β*-155 are schematically represented in Figure 2. The optimized geometry of α-84 is also presented for comparison.[8] The key geometric parameters are summarized in Table 1. (Detailed geometric information may be found in the Supporting Information.) The optimized structures have a coordinate RMS error of 0.71 Å to all atoms of the crystal structure,[10] indicating that the level of theory employed here is sufficient to describe geometric properties of the system. We noticed that the largest deviation from the crystal structure occurs at $C_{38}-C_{35}$. This, however, is the place where the incorporation of PCB into phytochromes is accomplished by the addition of a cystein side chain to the exo-cyclic double bond at ring A.[2]

Our calculations confirm the experimental finding that all three chromophores exhibit a similar geometry,[9,10] although there exist some subtle conformational differences. From C_{36} to C_{24} along the B, C rings, there are 12 C−C bonds altogether. For the $C_{36}-C_{11}$ bond, the optimized bond lengths are 1.3625, 1.3638, and 1.3655 Å for *β*-155, α-84, and *β*-84, respectively,

TABLE 1: Key Geometric Parameters for the Solution-Phase Optimized Model Complexes Consisting of $PCBH^+$ and the Asparate Residue as Shown in Figure 2

region	bond (Å)	α-84	β-84	β-155
A	$C_{38}-C_{35}$	1.3434	1.3449	1.3460
	$C_{34}-C_{35}$	1.5219	1.5219	1.5246
	$C_{35}-C_{36}$	1.4805	1.4805	1.4767
	$C_{36}-N_{32}$	1.3924	1.3907	1.3973
	$N_{32}-C_{33}$	1.3820	1.3837	1.3831
	$C_{33}-C_{34}$	1.5280	1.5265	1.5275
A−B	$C_{36}-C_{11}$	1.3638	1.3655	1.3625
	$C_{11}-C_{42}$	1.4377	1.4343	1.4481
B	$C_{42}-N_{41}$	1.3599	1.3571	1.3581
	$N_{41}-C_{45}$	1.3859	1.3854	1.3863
	$C_{45}-C_{44}$	1.4391	1.4453	1.4346
	$C_{44}-C_{43}$	1.3894	1.3854	1.3951
	$C_{43}-C_{42}$	1.4363	1.4415	1.4254
B−C	$C_{45}-C_{9}$	1.3905	1.3884	1.3994
	$C_{9}-C_{13}$	1.4036	1.4093	1.3957
	$C_{13}-N_{12}$	1.3843	1.3810	1.3832
	$N_{12}-C_{16}$	1.3628	1.3623	1.3590
	$C_{16}-C_{15}$	1.4251	1.4217	1.4344
	$C_{15}-C_{14}$	1.3986	1.4003	1.3902
	$C_{14}-C_{13}$	1.4301	1.4302	1.4392
C−D	$C_{16}-C_{10}$	1.4455	1.4461	1.4397
	$C_{10}-C_{24}$	1.3608	1.3603	1.3626
D	$C_{24}-C_{25}$	1.4766	1.4774	1.4780
	$C_{25}-C_{26}$	1.3594	1.3588	1.3587
	$C_{26}-C_{27}$	1.4871	1.4875	1.4866
	$C_{27}-N_{23}$	1.3914	1.3920	1.3948
	$N_{23}-C_{24}$	1.3929	1.3914	1.3910
A−B	$N_{32}-C_{36}-C_{42}-C_{43}$	−29.8	+27.1	−45.6
B−C	$N_{41}-C_{45}-C_{13}-N_{12}$	+18.3	+2.0	−11.3
C−D	$C_{15}-C_{16}-C_{24}-N_{23}$	−35.2	+31.5	+28.9

such that the bond lengths follow the trend β-155 < α-84 < β-84. For the neighboring $C_{11}-C_{42}$ bond, the optimized bond lengths are 1.4481, 1.4377, and 1.4343 Å, respectively; hence, the trend is β-155 > α-84 > β-84. Interestingly, the optimized bond lengths change alternatively to follow these two trends. Thus, it seems that the C−C bonds are more uniform along the B, C rings in α-84 than the other two. We relate this observation to more conjugation in α-84. Generally, more conjugation for a bilin produces lower energy for the first excited state.[1] Therefore, we expect that α-84 has an absorption maximum in the longer wavelength region.

By checking the optimized bond distances shown in Table 1, it is also clear that geometries are more similar to each other for α-84 and β-84 than for β-155. Thus, the maximum difference in bond length between α-84 and β-84 is 0.0062 Å, occurring at $C_{45}-C_{44}$, whereas the maximum difference in bond length between β-84 and β-155 is 0.0138/0.0136 Å, occurring at $C_{11}-C_{42}/C_9-C_{13}$.

Another interesting difference of these three chromophores lies in the relative orientation of the pyrrolic rings (see the dihedral angles listed in Table 1). For the optimized geometry of β-84, the B and C rings are practically in the same plane, as symbolized by $N_{41}-C_{45}-C_{13}-N_{12} = 2.0°$, while for those of α-84 and β-155, the B and C rings buckle to a certain degree in the opposite direction with $N_{41}-C_{45}-C_{13}-N_{12} = +18.3$ and $-11.3°$, respectively. We believe that the conjugation effect is enhanced when the B and C rings lie in the same plane, shifting the absorption maximum of β-84 to the longer wavelength region.

Assuming the B and C rings are roughly in the paper plane as shown in Figure 2, we find that, for the optimized geometry of β-84, ring D buckles up with the $N_{23}-H$ end with respect to ring B, while ring A buckles down with the $N_{32}-H$ end with respect to ring C. In contrast, for that of α-84, ring D buckles down with the $N_{23}-H$ end while ring A buckles up with the $N_{32}-H$ end with respect to the B, C rings, respectively. In the optimized geometry of β-155, both the $N_{23}-H$ and the $N_{32}-H$ ends buckle up with respect to the B, C rings, respectively. As compared to the crystal structures, there exist some subtle conformational differences.[10]

A factor which appears to play an important role in the spectroscopic properties of PCBs is the interaction between the asparatate residue and the B and C rings.[7,8,10] As ring C is protonated, the positive charge delocalizes over both ring C and ring B. Thus, we find that nitrogens in the B and C rings possess a similar negative charge for all three chromophores (Mulliken charges: around −0.77). We also find that the attached hydrogens possess a similar positive charge (Mulliken charges: around +0.41). The optimized geometries disclose that in β-84 and β-155 the ring B and ring C nitrogens act as donors for bifurcated hydrogen bonds with one of the carboxylate oxygens in the asparatate residues, while both carboxylate oxygens in the aspartate residue are invloved in the hydrogen bondings with the B and C rings in α-84.[8] Therefore, we find the charge distributions on the two carboxylate oxygens as −0.61/−0.63 (α-84) and −0.56/−0.64 (β-84 and β-155). For β-84 and β-155, a higher charge corresponds to a shorter O··H distance.

We find that solvent effects compress the bond lengths (see the Supporting Information for details). The optimization in PCM leads to the bond length which is usually shorter than the corresponding value obtained in the gas phase for the $PCBH^+$ moiety. However, the difference is normally smaller than 0.002 Å. The biggest difference is around 0.006 Å, which occurs at the $N_{32}-C_{33}$ and $C_{27}-N_{23}$ bonds of the A and D rings, respectively, in the structure unit of −NH−CO−. Larger geometric differences are encountered when using the neutral PCB model or the protonated PCB without the nearby asparatate residue (see the Supporting Information for details).

B. Spectroscopic Properties. For the α subunit, which contains one PCB, Mimuro et al. reported an absorption maximum at 618 nm with a clear shoulder around 570 nm. The separation of these two peaks was measured to be 48 nm.[5] Our previous calculations using TDDFT at the gas-phase optimized geometry led to the main absorption peak at 594 nm and the shoulder peak at 544 nm, with a separation of 50 nm between these two.[8] The updated numbers calculated at the solution-phase optimized geometry gave 594 nm for the main peak and 539 nm for the shoulder peak. The general agreement between theory and experiment lends credit to the reliability of our model and the methodology used here.

For the β subunit, the main absorption peak was measured to be at 606 nm with no clear shoulder around the main peak.[5] As the β subunit contains two PCBs of β-84 and β-155, Mimuro et al. separated the absorption spectrum into its component spectra by using a computer simulation based on a fitting of anisotropy.[5] These results are summarized in Table 2. Our calculated excitation spectra are also presented in Table 2. Superposition of the calculated peaks of β-84 and β-155 has been applied by using a Gaussian function. The superposed absorption spectrum shown in red in Figure 3b shows the maximum at 599 nm. No clear shoulder is discernible around the main peak. This well reproduces the observed absorption maximum (606 nm) of the β subunit in C-PC shown in Figure 3a.

The experimental CD spectra (Figure 3c) in the 300−650 nm region showed good correspondence to the absorption bands (Figure 3a). The maximum CD peak was observed at 582 nm,

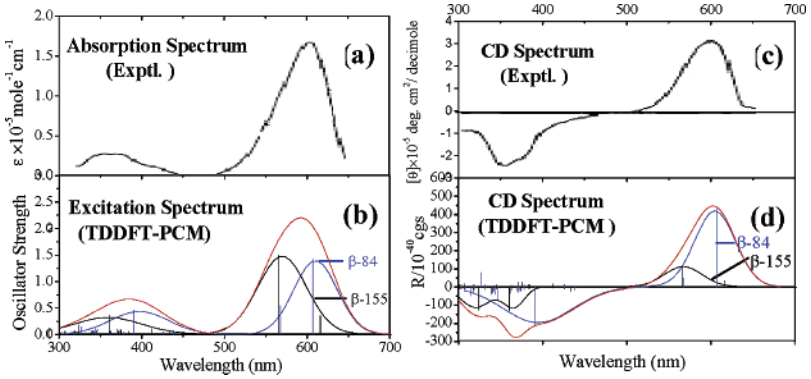

Figure 3. (a,c) Experimental absorption spectrum vs theoretical excitation spectrum at the level of TDDFT-PCM/6-31+G* for the β-subunit of C-PC. (b,d) Experimental CD spectrum vs theoretical CD spectrum at the level of TDDFT-PCM/6-31+G* for the β-subunit of C-PC. Black lines represent the theoretical spectra of β-155. Blue lines represent the theoretical spectra of β-84. Red lines represent the superposed spectra of both β-84 and β-155 PCBs. Gaussian expansions with width of 61 nm are applied to the theoretical absorption spectra and 47 nm to the theoretical CD spectra.

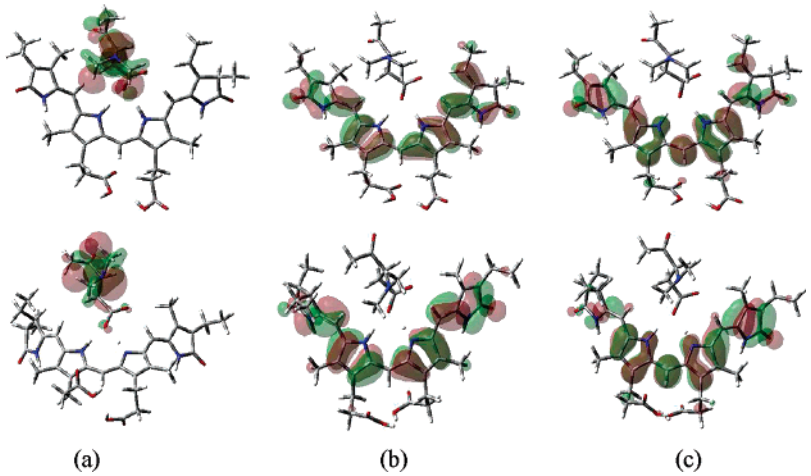

Figure 4. Contour maps for the frontier orbitals. The electron density of HOMO-1 orbital (a) is mainly from the aspartate residue, while those in HOMO (b) and LUMO (c) are composed of the aromatic π electrons of the pyrrole rings.

TABLE 2: Experimental Peaks (in nm) Observed in the Visible Absorption Region versus the Calculated Peaks at the TDDFT-PCM Level of Theory

		main peak	shoulder peak
α-84	calc.[a]	594	539
	exptl.[b]	618	570
β-84	calc.[a]	608	557
	exptl.[c]	624	565
β-155	calc.[a]	588	613
	exptl.[c]	594	550
β-84 + β-155	calc.[d]	599	N/A
	exptl.[b]	606	N/A

[a] Performed using B3LYP with the 6-31+G(d) basis set. [b] Observed in the absorption spectrum.[5] [c] Computer simulation based on a fitting of anisotropy.[5] [d] Superposition of the calculated peaks of β-84 and β-155 by a Gaussian function.

and some negative bands were observed between 300 and 450 nm, which implied that these bands came from different electronic transitions as compared to those of the red region bands.[5] Our theoretical CD spectrum (Figure 3d with the main peak of 582 nm) is also in good agreement with the experimental one (Figure 3c).

C-PC absorbs radiation in the regions of the visible spectrum where Chl *a* has low absorptivites; thus, the major interest is in the behavior and properties of the visible absorption band. The calculated singlet→singlet excited states summarized in Table 2 disclose some details of the β-84 and β-155 spectra, which are difficult to obtain directly from the experiment. For β-84, our calculations lead to the main peak (1^1A) at 608 nm with an oscillater strength of 1.38 and a blue-shifted shoulder peak (2^1A) at 557 nm with an oscillator strength of 1×10^{-4}. This is comparable to the computer fitting of the spectra of β-84, which indicated that the main peak and the shoulder peak were at 624 and 565 nm, respectively. For β-155, our calculations give the main peak (2^1A) at 588 nm with an oscillator strength of 1.44 and a red-shifted shoulder peak (1^1A) at 613 nm with an oscillator strength of 0.0198. Since the shoulder peaks of β-84 and β-155 are in close proximity to the main peaks of β-155 and β-84, respectively, with small oscillator strengths, it seems reasonable that no clear shoulder peak is observable in both the experimental and the theoretical spectra of the β subunit, which are the superposition of the spectra of the β-84 and β-155 chromophores. (Figure 3b,d).

Orbital analysis shows that the main peak of either β-84 or β-155 is mainly originated from the excitation from the highest occupied molecular orbital to the lowest unoccupied molecular orbital (HOMO → LUMO). The electron densities in these two frontier orbitals are composed of the aromic π electrons of the pyrrole rings (Figure 4b,c). The electron density of HOMO-1 orbitals, however, is from the aspartate residue (Figure 4a). Thus, the shoulder peak of either β-84 or β-155, whose main configuration is mainly originated from HOMO-1 → LUMO, is characterized as the charge transfer from the aspartate residue to $PCBH^+$. These findings are in line with our previous results for α-84.[8]

There are two mechanisms[1] which explain how energies are transferred among chromophores. In the strong coupling limit, exciton coupling may occur such that a pair of chromophores behave as if they are one unit, sharing delocalized energy.[1,7] On the other hand, in the weak coupling limit, the energy can be localized on one chromophore at a time such that the individual chromophores tend to retain their spectra.[1] Our calculations show that the absorption spectrum of the whole system can be reasonably well represented as the sum of its components. This result is indicative that Förster resonance theory in the weak coupling limit is predominant in the energy transfer between β-84 and β-155.[1] As the present calculations show that the wavelength of the main peak of β-155 lies at 588 nm, while that of β-84 lies at 608 nm, we may attribute β-155 to be the sensitizing chromophore (β_s) and β-84 the fluorescing chromophore (β_f) in the β subunit of C-PC. Thus, our calculations support the picture which also emerged from the experimental studies of Mimuro[5] and Suter et al.[17] that the energy transfer flow is light-sinked by β-155, which is then transferred to β-84 (cf. Figure 1).

We have optimized the structures in both the solution phase and gas phase and found that the $PCBH^+$ moiety experiences a slight change of the bond length as compared to the solution-phase structure to the gas-phase structure. Thus, the calculated main excitation is hardly affected as this peak comes mainly from the π electron excitation of the pyrrole rings. (The maximum shift (2 nm) occurs at β-84.) In comparison, PCM has a larger effect on the relative position between the $PCBH^+$ moiety and the asparate residue, which, in turn, will induce a significant change on the shoulder peak, as the shoulder peak arises mainly from the charge transfer from the asparate residue to $PCBH^+$. Indeed, adopting the PCM optimized geometries blue shifts the shoulder peaks by 5, 10, and 7 nm for α-84, β-84, and β-155, respectively. Thus, using the gas phase or PCM optimized geometry for β-84, we obtain a separation between the main peak and the shoulder peak of 39 or 51 nm. The latter is closer to the experimental value of 59 nm.[5] For β-155, our results put the main peak blue shift with respect to the shoulder peak, challenging the original assignment based on the computer fitting of the experimentally observed anisotropy.[5]

In line with our previous results for α-84,[8] we find that the effect of protonation of PCB is significant, which red-shifts the peak by around 50 nm for β-84 and β-155 (see the Supporting Information for details). Comparison between the theoretical spectra obtained from a given geometry with and without inclusion of PCM discloses the importance of the long-range interaction between the chromophore and the protein pocket. For example, without PCM, the main peak of β-84 is predicted at 580 nm, while the shoulder peak is predicted at 612 nm. Inclusion of PCM results in a red shift of the main peak by 26 nm and a blue shift of the shoulder peak by 45 nm, respectively. We also find that the solvation effect is more profound for β-155 and PCM leads to the same effect on the main peak and the shoulder peak. Hence, inclusion of PCM results in a red shift of the main peak by 25 nm and a blue shift of the shoulder peak by 100 nm, respectively (see the Supporting Information for details). Thus, our work shows that both the short- and the long-range interactions between the chromophore and the environmental protein moiety are very important.

IV. Conclusions

In summary, we present here a series of first-principle calculations at the TDDFT-PCM levels of theory to delineate the nature of the β-84 and β-155 PCBs in C-PC. We attribute the main peak for both β-84 and β-155 as arising from the π electron excitation of the pyrrole rings and the shoulder peak as arising from the charge transfer from the asparate residue to $PCBH^+$. The satisfactory agreement between theory and experiment suggests that Förster resonance theory prevails such that energy transfer occurs from β_s (β-155) to β_f (β-84).

Acknowledgment. This work was supported by the National Natural Science Foundation of China (No. 20525311, 20203009, 20021002, 20423002, 20533030), Natural Science Foundation of Hubei Province (No. 2005ABB012) for Distinguished Young Scholar, and the Ministry of Science and Technology of China (No. 2004CB719902, 2001CB61506, 2004CCA00100).

Supporting Information Available: Optimized geometrical parameters of model complexes for the β-84 and β-155 PCBs. This material is available free of charge via the Internet at http://pubs.acs.org.

References and Notes

(1) MacColl, R. *J. Struct. Biol.* **1998**, *124*, 311.
(2) (a) Braslavsky, S. E.; Schneider, D.; Heilhoff, K.; Nonell, S.; Aramendia, P. F.; Schaffner, K. *J. Am. Chem. Soc.* **1991**, *113*, 7322. (b) Smit, K.; Matysik. J.; Hildebrandt, P.; Mark, F. *J. Phys. Chem.* **1993**, *97*, 11887. (c) Guimaraes, C. R. W.; da Motta Neto, J. D.; Bicca de Alencastro, R. *Int. J. Quantum Chem.: Quantum Biol. Symp.* **1998**, *70*, 1145. (d) Debreczeny, M. P.; Sauer K.; Zhou J. H.; Bryant D. A. *J. Phys. Chem.* **1995**, *99*, 8412. (e) Debreczeny, M. P.; Sauer K.; Zhou J. H.; Bryant D. A. *J. Phys. Chem.* **1995**, *99*, 8420. (f) Strauss H. M.; Hughes, J.; Schmieder P. *Biochemistry* **2005**, *44*, 8244.
(3) Dale, R. E.; Teale, F. W. *J. Photochem. Photobiol.* **1970**, *12*, 99.
(4) Teale, F. W. J.; Dale, R. E. *Biochem. J.* **1970**, *116*, 161.
(5) (a) Mimuro, M.; Fuglistaller, P.; Rumbeli, R.; Zuber, H. *Biochim. Biophys. Acta* **1986**, *848*, 155. (b) Mimuro, M.; Rumbeli, R.; Fuglistaller, P.; Zuber, H. *Biochim. Biophys. Acta* **1986**, *851*, 447.
(6) Kikuchi, K.; Sugimoto, T.; Mimuro, M. *Chem. Phys. Lett.* **1997**, *274*, 460.
(7) (a) Scharnagl, C.; Schneider, S. *J. Photochem. Photobiol. B: Biol.* **1989**, *3*, 603. (b) Scharnagl, C.; Schneider, S. *J. Photochem. Photobiol. B: Biology* **1991**, *8*, 129.
(8) Wan, J.; Xu, X.; Ren, Y. L. *J. Phys. Chem. B* **2005**, *109*, 11088.
(9) Schirmer, B. W.; Huber, R. *J. Mol. Biol.* **1987**, *196*, 677.
(10) Durring, M.; Schmidt, G. B.; Huber, R. *J. Mol. Biol.* **1991**, *217*, 577.
(11) Frisch, M. J.; Trucks, G. W.; Schlegel, H. B.; Scuseria, G. E.; Robb, M. A.; Cheeseman, J. R.; Montgomery, J. A., Jr.; Vreven, T.; Kudin, K. N.; Burant, J. C.; Millam, J. M.; Iyengar, S. S.; Tomai, J.; Barone, V.; Mennucci, B.; Cossi, M.; Scalmani, G.; Rega, N.; Petersson, G. A.; Nakatsuji, H.; Hada, M.; Ehara, M.; Toyota, K.; Fukuda, R.; Hasegawa, J.; Ishida, M.; Nakajima, T.; Honda, Y.; Kitao, O.; Nakai, H.; Klene, M.; Li, X.; Knox, J. E.; Hratchian, H. P.; Cross, J. B.; Adamo, C.; Jaramillo, J.; Gomperts, R.; Stratmann, R. E.; Yazyev, O.; Austin, A. J.; Cammi, R.; Pomelli, C.; Ochterski, J. W.; Ayala, P. Y.; Morokuma, K. G.; Voth, A.; Salvador, P.; Dannenberg, J. J.; Zakrzewski, V. G.; Dapprich, S.; Daniels, A. D.; Strain, M. C.; Farkas, O.; Malick, D. K.; Rabuk, A. D.; Raghavachari, K.; Foresman, J. B.; Ortiz, J. V.; Cui, Q.; Baboul, A. G.; Clifford, S.; Cioslowski, J.; Stefanov, B. B.; Liu, G.; Liashenko, A.; Piskorz, P.; Komaromi, I.; Martin, R. L.; Fox, D. J.; Keith, T.; Al-Laham, M. A.; Peng, C. Y.; Nanayakkara, A.; Challacombe, M.; Gill, P. M. W.; Johnson, B.; Chen, W.; Wong, M. W.; Gonzalez, C.; Pople, J. A. Gaussian 03, Revision B.03; Gaussian, Inc., Pittsburgh, PA, 2003.
(12) (a) Becke, A. D. *J. Chem. Phys.* **1993**, *98*, 5648. (b) Becke, A. D. *Phys. Rev. A* **1988**, *38*, 3098. (c) Slater, J. C. *Quantum Theory of Molecular and Solids, Vol. 4, The Self-Consistent Field for Molecular and Solids*; McGraw-Hill: New York, 1974. (d) Vosko, S. H.; Wilk, L.; Nusair, M. *Can. J. Phys.* **1980**, *58*, 1200. (e) Lee, C.; Yang, W.; Parr, R. G. *Phys. Rev. B* **1988**, *37*, 785.
(13) Ditchfield. R.; Hehre, W. J.; Pople, J. A. *J. Chem. Phys.* **1971**, *54*, 724.
(14) (a) Cossi, M.; Barone, V. *J. Chem. Phys.* **2001**, *115*, 4708. (b) Mierus, S.; Scrocco, E.; Tomasi, J. *J. Chem. Phys.* **1981**, *55*, 117. (c) Barone, V.; Cossi, M.; Tomasi, J. *J. Chem. Phys.* **1997**, *107*, 3210.
(15) Blomberg, M. R. A.; Siegabahn, P. E. M.; Babcock, G. T. *J. Am. Chem. Soc.* **1998**, *120*, 8812.
(16) We thank the referee for proposing to check this possibility.
(17) Suter, G. W.; Mazzola, P.; Wendler, J.; Holzwarth, A. R. *Biochim. Biophys. Acta* **1984**, *766*, 269.